SPECIAL GUEST EDITOR SECTION

Dye Removal from Water and Wastewater Using Various Physical, Chemical, and Biological Processes

KRZYSZTOF PIASKOWSKI, RENATA ŚWIDERSKA-DĄBROWSKA, and PAWEŁ K. ZARZYCKI[1]
Koszalin University of Technology, Faculty of Civil Engineering, Department of Environmental Technologies and Bioanalytics, Environmental and Geodetic Sciences, Sniadeckich 2, Koszalin, Poland 75-453

Synthetic dyes or colorants are key chemicals for various industries producing textiles, food, cosmetics, pharmaceutics, printer inks, leather, and plastics. Nowadays, the textile industry is the major consumer of dyes. The mass of synthetic colorants used by this industry is estimated at the level of $1 \div 3 \times 10^5$ tons, in comparison with the total annual consumption of around 7×10^5 tons worldwide. Synthetic dyes are relatively easy to detect but difficult to eliminate from wastewater and surface water ecosystems because of their aromatic chemical structure. It should be highlighted that the relatively high stability of synthetic dyes leads to health and ecological concerns due to their toxic, mutagenic, and carcinogenic nature. Currently, removal of such chemicals from wastewater involves various techniques, including flocculation/coagulation, precipitation, photocatalytic degradation, biological oxidation, ion exchange, adsorption, and membrane filtration. In this review, a number of classical and modern technologies for synthetic dye removal from industry-originated wastewater were summarized and discussed. There is an increasing interest in the application of waste organic materials (e.g., compounds extracted from orange bagasse, fungus biosorbent, or green algal biomasses) as effective, low-cost, and ecologically friendly sorbents. Moreover, a number of dye removal processes are based on newly discovered carbon nanomaterials (carbon nanotubes and graphene as well as their derivatives).

More than 3000 textile dyes are currently synthesized and used in various industrial processes. Additionally, dye production, dyeing, or printing involve more than 8000 supplementary chemicals (1). In the last decade, consumption of synthetic dyes has been rapidly increasing, particularly in the textile industry. It has been estimated that more than 2×10^5 tons per year of textile dyes may be discharged worldwide (2). The presence of colored substances in water is unacceptable in terms of human consumption (3). It should be noted that up to 15% of the dyes mass produced may be lost in the effluents during the dyeing process (4). It has been reported that inappropriate and uncontrolled release of textile effluents to the environment, especially to surface water ecosystems, may cause serious and long-term water pollution, which may put approximately 1 million people at risk (5). It should be noted that dyes and colorants are still poorly characterized in terms of ecotoxicological risk. Due to the significant amount of colorants that is estimated to be lost to waste streams and is nonprocessed by conventional wastewater treatment, they must be considered potentially hazardous for organisms living in fresh water aquatic ecosystems. The latest studies of aquatic toxicity, focusing on 42 commercial synthetic colorants for textile dyeing, have indicated that algae can be more sensitive to colorants in comparison with daphnids, particularly if the effect of biomass were analyzed (6).

Synthetic dyes can be classified into several categories based on their chemical structure and presence of chromophores and/or auxochrome groups, such as azo, anthraquinone, sulfur, indigo, triphenylmethyl, and phthalocyanine derivatives (Figure 1). The presence of auxochromes may increase the intensity of dye color. Moreover, to increase their solubility in water, acidic groups are often incorporated into the dye structure, including the sulfonic group (SO_3H) or the carboxylic group (COOH). They are usually used as sodium salts.

The most important class of commercial dyes and versatile colorants are azo dyes. Due to their wide variety of color shades, high wet fastness profiles, and easy and low-cost production, these colorants have been used excessively in industries worldwide, particularly in comparison with natural dyes (7, 8).

Textile effluents are considered highly toxic due to the presence of parent compounds and their degradation products containing aromatic rings and reactive groups such as sulfur, naphthol, and nitrates, as well as heavy metals like copper, arsenic, lead, cadmium, mercury, nickel, cobalt, and chromium. Additionally, dyeing processes involve harmful supplementary chemicals that may be transferred to wastewater, including organic acids, surfactants (e.g., soaps, hydrocarbon-based softeners), formaldehyde-based dye fixing agents, chlorinated stain removers, and other nonbiodegradable dyeing chemicals. These substances may react with common disinfectants, especially chlorine, and form a number of disinfection byproducts, which are often carcinogenic and/or may cause allergic reactions (1). In water ecosystems, the chemical structure of dyes can be modified, resulting in the formation of new compounds that can be even more toxic (9). Another environmental risk concerning the presence of dyes in surface water ecosystems is associated with high absorbance of sunlight causing a decrease in the photosynthetic activity of phytoplankton (10). It has been found that dyes and related pollutants present in surface water can be transferred to food (11). Recently, it has been documented that long-term consumption of water containing dyes may affect the bodies of both animals and humans, particularly the digestive and central nervous systems, leading to their severe damage (12, 13).

Guest edited as a special report on "Analysis and Applications of Colorants and Optical Sensing Markers" by Paweł K. Zarzycki.

[1]Corresponding author's e-mail: pkzarz@wp.pl

DOI: https://doi.org/10.5740/jaoacint.18-0051

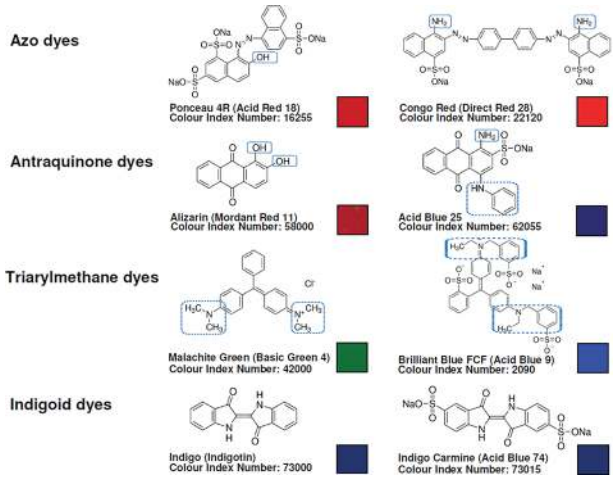

Figure 1. Chemical structures and color indexes of selected synthetic dyes, with highlighted auxochromes. Color figures are available online as supplemental information at: http://aoac.publisher.ingentaconnect.com/content/aoac/jaoac

Removal of Dyes from Water/Wastewater—Processes Overview

Dyes-originated pollutants that are present in textile wastewater may change the key parameters reflecting wastewater quality, including suspended and dissolved solids, biological oxygen demand, and chemical oxygen demand. The stability and low biodegradability of dyes and related molecules result in many technological problems during wastewater treatment (14–16).

Currently, there are two main streams of textile wastewater treatment: (*1*) Dyes are transferred into solid phase or sludge biomass and (*2*) mineralized using, e.g., chemical and biological oxidation (9; Figure 2). Modern wastewater treatment may be based on simple or hybrid physical and chemical processes such as adsorption, coagulation/flocculation, chemical and electrochemical oxidation, ozonation, ion exchange, membrane process, filtration with coagulation, ozonation with coagulation and adsorption, photocatalysis, sonication, and irradiation (2, 15, 17). A number of efficient dye removal systems (e.g., consisting of coagulation and sorption processes) involve high-cost reagents and may generate additional hazardous waste (2). On the other hand, complete dye removal may be achieved using a number of advanced oxidation technologies, in which nonselective hydroxyl radicals are generated (e.g., ozonation, Fenton's processes, electrochemical destruction, and photocatalysis). Unfortunately, they require fairly complicated procedures, which increase the total cost of micropollutant removal (9). Another alternative method is biodegradation (biological decomposition processes), in which target pollutants can be completely mineralized. Such technology allows for a decrease in the total cost of wastewater treatment. These methods are more ecologically friendly because aggressive chemicals are usually not required (15, 17).

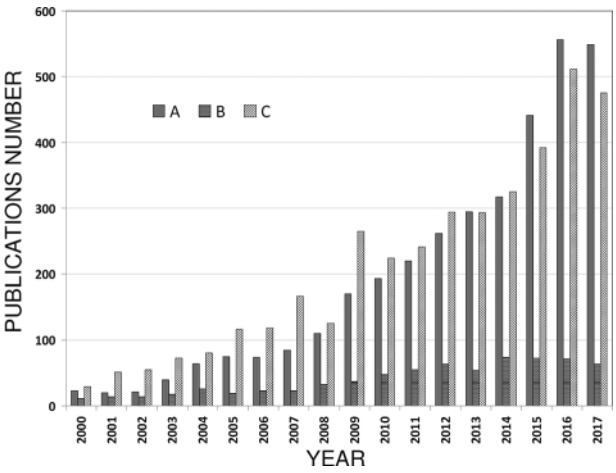

Figure 2. Comparison of the number of manuscripts available through the Web of Science database. Topic key words: (A) "dye" and "wastewater" and "adsorption," (B) "dye" and "wastewater" and "biodegradation," and (C) "dye" and "wastewater" and "coagulation" or "oxidation" or "membrane."

Generally, there is an increasing interest in research focusing on the effective removal of dye-related micropollutants from wastewater based on (*1*) adsorption, (*2*) biodegradation and biosorption, and (*3*) coagulation, membrane separation, and oxidation processes (Figure 3).

Adsorption Processes

Adsorption is one of the most efficient and commonly used purification processes for wastewater treatment. Typical adsorption-driven dye removal methods that were reported in currently published publications are summarized in Table 1 (18–28). Generally, adsorption can be applied to remove dyes and other organic as well as inorganic pollutants, including micropollutants, in large-scale wastewater technology. Activated carbon-based materials are the most commonly used adsorbents due to their high efficiency and the simple technology involved. However, these materials are characterized by high production cost and low degree of regeneration. For that reason, there is extensive research focusing on the invention of more efficient and recyclable sorbents, which may replace classical active carbons (25). They are composed of both natural and synthetic materials, e.g., clay minerals (29), metal oxides (26), polymers (24), composites (18, 23), and food waste (28, 19). There is great interest in the use of various magnetic nanomaterials as sorbents because of their easy separation after the adsorption process and their high efficiency, primarily due to high surface-to-volume ratio (20, 26, 30). Most recently, one such approach was studied by Moawed and coauthors (21). They coupled magnetic nanoparticles based on iron (II,III) oxide (Fe_3O_4) with commercial polyurethane foam through isothiouronium groups. They prepared a porous sorbent with improved ionic properties and better sorption affinity toward ionic molecules. This enabled them to remove both cationic (Brilliant Green) and anionic (Brilliant Yellow) dyes from the liquid phase in a wide range of solution pH values. The presence of magnetic particles (21.4 nm particle size) in the described purification system allowed rapid removal of active sorbent from the liquid phase by applying an external magnetic field (21). In the experiment described by Wang et al., a hybrid adsorbent was tested (23). They prepared magnetic β-cyclodextrin-graphene oxide nanocomposites that were successfully applied for the removal of cationic dye (Malachite Green). Graphene oxide has been found to possess excellent adsorption properties due to a large surface area and the presence of a number of polar

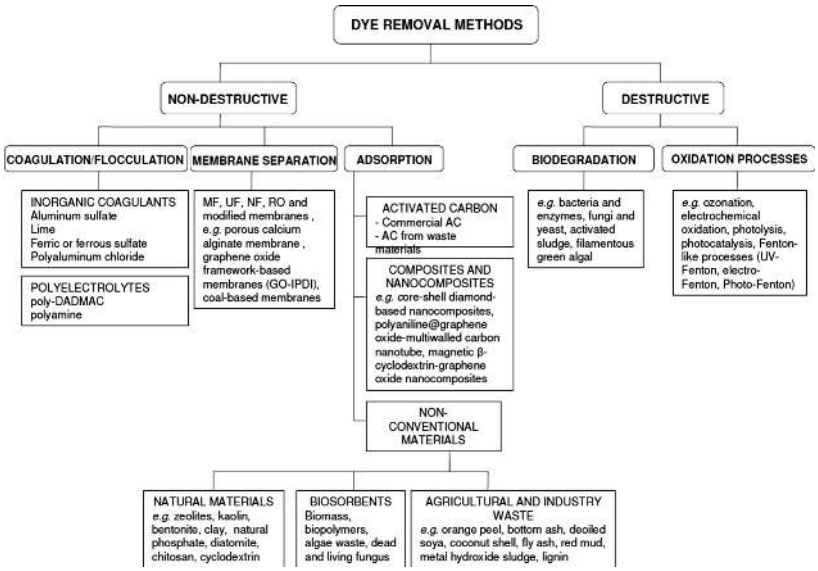

Figure 3. General scheme of dye removal processes using various treatment methods.

Table 1. Removal of dyes from water solutions/wastewater through the adsorption process

Target compound	Experiment setup	Quantification protocols	Complementary data	Ref.
Rhodamine B Methylene Blue	The core-shell diamond-based nanocomposites were synthesized in several steps: First, diamond-graphite was oxidized to diamond-graphene oxide composite, and carboxyl groups from chloroacetic acid were then attached to it. Finally, material was immersed alternately in the aqueous solution of polyethylenimine and poly acrylic acid in order for the formation of adsorption layers on the diamond surface (maximum of 12 cycles). Batch method: 50 mL aqueous solution of dye (10 mg/L for Methylene Blue and 5 mg/L for rhodamine B) with 10 mg of adsorbent was stirred in a dark condition at room temperature.	Analysis of dyes concentration using UV-Vis spectrophotometer (554 nm for rhodamine B and 662 nm for Methylene Blue).	Fabricated composite shows high adsorption capacity toward the dyes used. Adsorbent can be easily separated from wastewater and repeatedly used to remove dyes.	(18)
Acid Red 18, Acid Orange 7, Acid Black 1—anionic azo dyes	The wheat bran modified with cationic gemini surfactant (N1-dodecyl-N1, N1, N2, N2-tetramethyl-N2-octylethane-1,2-diamonium bromide, 12-2-12). Batch method: NA[a]	Analysis of dyes concentration using UV-Vis spectrophotometer (510, 490, and 610 nm, for Acid Red 18, Acid Orange 7, and Acid Black 1, respectively).	The adsorption performance strongly depends on pH of solution and its ionic strength (pH < 3, salinity < 0.4 mol/L NaCl). The interaction between anionic dyes and adsorbent depends on type of dye: The adsorption of Acid Red 18 and Acid Orange 7 was endothermic and spontaneous, whereas the adsorption of Acid Black 1 was exothermic.	(19)
MB[b], MV[c], BG[d], RhB[e]	The magnetic carboxyl-functionalized attapulgite/carbon nanocomposites were fabricated from the spent bleaching earth by one-pot hydrothermal method in the presence of ferric chloride and sodium citrate. Batch method: 20 mL aqueous solution of dye (100 mg/L) with 20 mg adsorbent was stirred (160 rpm) at a constant temperature of 25°C.	Separation of the adsorbent by magnetic technique and spectrophotometric analysis of dyes and lead at 533, 665, 582, 624, and 554 nm for Pb(II), MB, MV, BG, and RhB, respectively.	Sorption and magnetic properties of the resultant adsorbents strongly depends on concentration of sodium citrate—optimum 0.6 mol/L. Under these conditions, highest adsorption capacity (254.83 mg/g for MB) was obtained. The adsorbent can be easily recycled due to its magnetism and a slight decrease of adsorption capacity in subsequent cycles.	(20)
Brilliant Yellow (anionic dye) and Brilliant Green (cationic dye)	The magnetite porous sorbent, prepared from commercial polyurethane foam, which was coupled with Fe_3O_4 through isothiouronium groups. Batch method: 25 mL aqueous solution of dye (1 g/L) with 0.1 g adsorbent was shaken for 1 h at a variable temperature (30–65°C) and pH of solution (1–12). Dynamic experiments: 1.0 g adsorbent packed into a glass column (d = 1.5 cm), 25 mL dye solution (1 mg/L), a flow rate of 2 mL/min.	Separation of dye by filtration and then spectrophotometric analysis.	Adsorbent had acidic character and is stable both in acidic and alkaline solutions. High sorption efficiency was achieved at optimum pH value, both for Brilliant Yellow and Brilliant Green (capacity 328 and 225 mg/g, respectively).	(21)

Table 1. (*continued*)

Target compound	Experiment setup	Quantification protocols	Complementary data	Ref.
Congo Red	Polyaniline@graphene oxide-multiwalled carbon nanotube composite, prepared by an in situ polymerization methodology, and finally doped with para toluene sulfonic acid to generate additional functionality. Batch method: 20 mL aqueous solution of dye and Cr(VI) with 20 mg adsorbent was shaken at a variable temperature and pH of solution.	Analysis of dye concentration using UV-Vis spectrophotometer at 495 nm.	The adsorption performance strongly depends on pH of solution—the max adsorption was observed in an acidic medium at 30°C. .The resultant adsorbent can be used to remove both dye and heavy metals from industrial wastewaters.	(22)
Malachite Green (cationic dye)	The magnetic β-cyclodextrin-graphene oxide nanocomposites. Batch method: 20 mL aqueous solution of dye (5–800 mg/L) with 5 mg adsorbent was shaken for 2 h at a variable temperature (25–45°C) and pH of solution (4–9).	Separation of the adsorbent using external magnet field and spectrophotometric analysis of dye concentration at 618 nm.	The adsorbent can effectively remove dyes from wastewater—the maximum adsorption capacity was 990.10 mg/g at 45°C and pH 7. It can be repeatedly used thanks to its stability (after five cycles, the adsorption capacity only decreased by 20%) and magnetism (ease of separation).	(23)
Ponceau 4R (azo dye)	The insoluble polyamidoamine–cyclodextrin crosslinked copolymer (PAMAM-CD). Batch method: 50 mL aqueous solution of dye (130–350 mg/L, pH 5) with 50 mg PAMAM-CD was shaken (60 rpm) up to 12 h at set temperature (15–35°C). Effect of pH in range 2–7 on the adsorption of dye was also determined.	Separation of dye by centrifugation and spectrophotometric analysis at 508 ± 2 nm.	The process was fast and spontaneous. Maximum adsorption capacity (254.3 mg/g) was achieved at the initial concentration of dye 340 mg/L, temperature 15°C, and at pH below 5. The PAMAM-CD was easily recovered by 2 M HCl as washing solvent.	(24)
Methyl Violet (cationic dye)	The SBA-15 mesoporous silica. Batch method: 50 mL aqueous solution of dye (10–40 mg/L, pH 8) with 0.2 g adsorbent was stirred (150 rpm, 5 min) at a constant temperature of 25°C.	Separation of dye by centrifugation (2000 rpm, 3 min) and determination of dye concentration using Image-Pro Plus software and UV-Vis spectroscopy (for comparison).	The sorption was fast and very effective; removal of the dye was 99% after 5 min of contact at pH 8. Results obtained using two methods of quantification of Methyl Violet were consistent; maximum relative error was 1.83%.	(25)
Reactive Orange 13 and Reactive Yellow 15 (anionic dyes)	The iron oxide nanospheres—ferromagnetic particles with radius <75 nm, synthesized with the solvothermal method. Batch method: 5 mL aqueous solution of dye (20–80 mg/L, pH 7) with 5 mg adsorbent was stirred (150 rpm) at a constant temperature of 25°C. The influences of solution pH (4–10.5) and temperature (25–55°C) were also determined.	Separation of adsorbent by a strong permanent magnet and spectrophotometric analysis of dye concentration.	The process of sorption was rapid (mainly took place within 10 min) and efficient, especially in acidic solution. The maximum adsorption capacity for Reactive Orange and Reactive Yellow were 32.5 and 25.0 mg/g, respectively. Because of its magnetism, the adsorbent can be easily separated and reused.	(26)
Rhodamine 6G (cationic dye) and Congo Red (anionic dye)	Moroccan natural phosphate; contains 98 wt % fluoroapatite $Ca_5(PO_4)_3F$. Batch method: 20 mL aqueous solution of dye (100–400 mg/L) with or without NaCl, with 1–30 g/L adsorbent, was stirred (400 rpm) at room temperature within 5–300 min. Solution pH was 3–12.	The concentration of dyes was analyzed using UV/VIS/NIR[f] spectrometer at 526 and 497 nm for Rhodamine 6G and Congo Red, respectively.	The natural phosphate could be a good adsorbent both for cationic and anionic dyes from industrial wastewater with low salinity (<100 mM NaCl). The obtained max. adsorption capacity at pH 5.2 was 6.84 and 19.81 mg/g for Rhodamine 6G and Congo Red, respectively.	(27)
Methylene Blue	Pectin and pectin/cellulose microfibers beads, which were synthesized using compounds extracted from orange bagasse via physical crosslinking with calcium ions. Batch method: 50 mL aqueous solution of dye (10–500 mg/L) with 20 mg adsorbent was stirred at room temperature. Desorption of dye in mixture 1 M HCl and ethanol (1+1).	The concentration of dye was determined using a UV-Vis spectrophotometer at 670 nm.	Microfibers, synthesized from the food industry organic residue, are low-cost, eco-friendly, and efficient adsorbents toward organic dye. Maximum adsorbent capacity was 1550.3 mg/g for pectin microfibers and 2307.9 mg/g for pectin/cellulose microfibers.	(28)

[a] NA = Not available.

[b] MB = Methylene Blue.

[c] MV = Methylene Violet.

[d] BG = Brilliant Green.

[e] RhB = Rhodamine B.

[f] NIR = Near-infrared.

hydroxyl, epoxide, and carboxylic groups. This is also the reason that such carbon-based nanomaterial was well dispersed in water. An additional component of the described hybrid sorbent, namely native β-cyclodextrin (β-CD), has a unique physicochemical property due to its geometry and chemical structure. Generally, cyclodextrins are donut-shaped molecules, which are characterized by a nonpolar internal cavity and a polar external surface. Therefore, they are soluble in polar liquids (e.g., water, dimethyl sulfoxide) or binary water–organic liquid mixtures (e.g., acetonitrile–water, ethanol–water; 31). These properties allow for the creation of selective host–guest complexes (also in terms of enantioselectivity) with various low-molecular-mass compounds. In particular, β-cyclodextrin may adsorb both organic and inorganic micropollutants from wastewater matrices. This process is more effective at subambient temperatures (31). Purification systems involving macrocyclic compounds or polysaccharide-based materials revealed outstanding removal capabilities for certain micropollutants, especially for antibacterial drugs and organic endocrine disrupters as well as for various colorants (24, 28, 32–38). Trace quantities of endocrine-disrupting compounds and pharmaceuticals are very difficult to remove from complex matrices such as wastewater using classical technologies involving commonly applied sorbents or commercial-activated carbons. In the experiment by Wang and coauthors, the presence of cyclodextrin increased the adsorption capacity of hybrid material tested for Malachite Green dye. They have reported that the maximum adsorption capacity of the target pollutant was around 990 mg/g at 45°C and pH = 7 (23).

Most recently, mesoporous silica (e.g., SBA-15) has been found to be a very promising sorption material characterized by specific porous structure and excellent textural properties facilitating diffusion of dye molecules. It has been proved that SBA-15 may exhibit efficient sorption for Methyl Violet. For example, almost 99% of dye can be removed from an aqueous solution at pH = 8 after a relatively short contact time of 5 min (25).

There is an increasing interest in wastewater purification by the application of food waste sorbents. Postprocessed fruits and vegetables involving seeds, peels, and pulps have been tested. These materials were previously treated as common waste without additional industrial applications (28), although it has now been documented that they can be a source of many functional compounds for wastewater processes. For example, orange pulp is mainly composed of polysaccharide-based chemicals like cellulose, hemicellulose, pectin, and small amounts of lignin, which may be applied as efficient sorbents. Lessa et al. reported an extraction protocol of cellulose and pectin from orange pulp waste and then the reuse of such biomaterials to synthesize the pectin and pectin/cellulose microfibers beads. Using the described technology, they obtained eco-friendly sorbent, which is effective for Methylene Blue pollutant. The surface of cellulose microfibers is characterized by a number of hydroxyl groups that may interact with dye molecules by electrostatic forces. The chemical structure of cellulose microfibers results in high efficiency of sorption. Particularly, the maximum adsorption capacity of such material was calculated as 1550 mg/g for pectin microfibers and 2308 mg/g for pectin/cellulose microfibers (28).

In particular cases, biomass-originated adsorbents should be modified through appropriate derivatization or physicochemical treatment to achieve high adsorption efficiency. For instance, Zhang and coauthors modified wheat bran with gemini-type surfactant to remove anionic azo dyes (Acid Red 18, Acid Orange 7, and Acid Black 1) (19). Ge and coworkers grafted maleic anhydride onto sugarcane bagasse. Such modified biomaterial was then used to remove Methylene Blue from wastewater (39). Of note, food industry–generated waste can be used for the preparation of porous carbonaceous materials characterized by selective adsorption properties. Such biomaterial can be prepared from vegetable residues (prickly pear peels, broccoli stems, white sapote seeds; 40) or fish scales (41). To increase their porosity, such products must be chemically activated, usually involving phosphoric acid treatment.

Biodegradation and Biosorption Processes

Biological methods are an interesting alternative for dye removal from wastewater. They can be based on activated sludge containing various aerobic and anaerobic microorganisms including fungi, bacteria, and green algae. Some recently developed technologies involve more advanced processes using, e.g., isolated bacterial enzymes. At this time, such systems are extensively studied and employed as efficient methods for the purification of dye-polluted wastewater (Table 2). Generally, the application of microorganism-driven purification processes has many advantages, such as relatively low cost, small amount of sludge production, and the discharging of nontoxic mineralization substances. It has been reported that biological processes have great potential to convert or degrade dye-related contaminations into water, carbon dioxide, and various inorganic salts. Biological processes are usually environmentally friendly and can also be adapted for wastewater technological processes working under strict green chemistry principles (7, 9).

Dye bioremediation can be achieved via biosorption and/or biodegradation. These processes involve different removal mechanisms for given pollutants. Biosorption is based on the biomaterials–colorants interactions where colorants are physically or chemically attached to the biomass surface. Such interactions may include absorption, adsorption, diffusion, ion exchange, chelation, surface complexation, and precipitation. Moreover, dye biosorption involves interactions with various ligands that may be present on both the biomaterial surface and dye structures, e.g., carboxylic, hydroxyl, amino, carbonyl, phosphate, and sulfonic groups. During biodegradation, contaminants are degraded by enzymes that are present in various fungi- or bacteria-composed biomass (10, 11, 44). The most significant factors that influence the effectiveness of biological dye removal are related to adaptability and activity of microorganisms (45).

Research carried out by Buntić and coauthors (9) has shown the capabilities of the *Streptomyces microflavus* CKS6 microorganism in the treatment of textile wastewater containing Crystal violet (CV) and Safranin T (ST) dyes. The reported protocol enabled wastewater bioremediation that is safe for the environment. This protocol was performed in two subsequent steps: dye adsorption onto the bacterial surface and complete biodegradation by the microorganism's enzymatic system. Various decolorization rates were observed depending on the experiment conditions (temperature, dye concentration, and pH). Particularly, more than 80 and 90% of decolorization for ST and CV was obtained, respectively. The authors indicated that

Table 2. Removal of dyes from water solutions/wastewater through biodegradation and/or biosorption processes

Target compound	Experiment setup	Quantification protocols	Complementary data	Ref.
Anthraquinone dye: Alizarin Blue Black B	Biosorption by microscopic fungi: *Haematonectria haematococca* BwIII43, K37, and *Trichoderma harzianum* BsIII33. Source of fungi: isolation from the soil. Optimal conditions of the biosorption process: 1 g mycelium biomass/50 cm^3 liquid medium with 0.03% dye, pH = 7.0, 28°C.	Separation by centrifugation (6000 rpm) and spectrophotometric analysis of the dye concentration (526 nm).	The highest sorption capacity after 7 days in optimal conditions by the *H. haematococca* K37–247.05 mg/g.	(11)
Indigo, Remazol Brilliant Blue R, Sulphur Black, and the dye-containing liquid effluent	Biodegradation by the cyanobacteria *Anabaena flos-aquae* UTCC64[a], *Phormidium autumnale* UTEX1580[b] and *Synechococcus* sp. PCC7942[c] compared with anaerobic and anaerobic–aerobic systems. Conditions of the process: synthetic dyes concentration 0.02% (m/v), 50 mL AA[d] or BG-11[e] culture media, 1 mL the cyanobacterium culture medium, incubating for 14 days at 25°C with constant fluorescent illumination (4000 ± 10% lux). An anaerobic–aerobic degradation condition for dye discoloration in the liquid wastewater: 15 days at 28°C in the dark and then aerobically incubating in the same conditions.	Centrifugation after the process at 10 000 × *g* for 5 min. and absorption maximum for each dye was 680 nm (indigo), 595 nm (Remazol Brilliant Blue R), and 454 nm (Sulphur Black).	Percentage of dyes discoloration: Anabaena sp.: Indygo—72%, Remazol Brilliant Blue R—0%, Sulphur Black—42%. Phormidium sp.: Indygo—91%, Remazol Brilliant Blue R—11%, Sulphur Black—0%. Synechococcus sp.: Indygo—0%, Remazol Brilliant Blue R—11%, Sulphur Black—0%. In the anaerobic–aerobic system, dye discoloration in the liquid wastewater after anaerobic treatment—17 and 33% after combined anaerobic–aerobic.	(42)
Congo Red and Gentian Violet	Biodegradation by extracellular bacterial laccases enzyme producing *Pseudomonas stutzeri* MN1[f] and *Acinetobacter baumannii* MN3. Source of laccase-producing bacteria: isolation from crude oil. Conditions of the process: incubating laccase-producing bacterium and crude laccase (culture filtrate) at 37°C with concentration 100–500 ppm of each dye for 1–5 days.	Centrifugation (10 000 g at 4°C for 10 min) from the overnight cultures and culture supernatant measuring the decolorization of synthetic dyes by UV spectrophotometer.	Congo Red decolorized by MN1 in 84%, by MN3 in 89%. Mixed consortia (MN1 + MN3)—97% decolorization efficiency on fifth day. Gentian Violet decolorized by MN1 in 83%, by MN3 in 90% and (MN1 + MN3) in 95% on fifth day.	(2)
Synthetic single and double azo dyes: Orange II, Amido Black 10B, Ponceau S, Congo Red, Acridine Orange, Coomassie Brilliant Blue, Cibacron Navy DP-B, Remazol Brilliant Blue R	Enzymatic decolorization by acidic horseradish peroxidase. Source of HRP-A—isolation from the fresh roots of horseradish. Dye solutions prepared from the powdered dyes as stock solution (2 mg/mL) in phosphate-buffered saline. Conditions of the process: dye solution 300 µg/mL, 20 µL 3 U/mL HRP-A and 170 µM H_2O_2. 1 h incubating in room temperature (25°C) in the dark.	Measurements of the effectiveness of decolorization based on the UV-Vis absorption spectra (from 200 to 800 nm in 1.0 cm quartz cells).	The rate of decolorization: Orange II—93.5%, Amido Black 10B—83.25%, Ponceau S—56.7%, Congo Red—53.7%, Acridine Orange—45.6%, Coomassie Brilliant Blue—76%, Cibacron Navy DP-B—68.5%, Remazol Brilliant Blue R—71.7%.	(16)
CV and ST	Biodegradation of dyes by bacterium *Streptomyces microflavus* CKS6[g] isolated from forest soil. Decolorization of solution containing basic dyes (CV and ST). Incubating of the CKS6 cells with 25 mL dyes solution, in the ratio of 1:10 (v:v). Shaking under the aeration of 120 rpm. The initial solutions of CV and ST dyes (1–30 mg/L). Time reaction: 12–24 h.	Separating from bacterial cell mass by centrifugation at 10 000 × *g* for 10 min.Color reduction in supernatant measuring by UV-Vis spectroscopic monitoring analysis at 584 (CV) and 554 nm (ST).	A possible mechanism of decolorization: 1—dye adsorption onto the bacterial cells surface, 2—biodegradation by the active microbial enzymatic system (by the lignin peroxidase). Optimized process parameters: reaction temperature (27–30°C) and pH 6–7. With increasing dye concentration from 1 up to 30 mg/L, the CV decolorization percentage declined from 100.0 to 46.7% and ST from 83.1 to 29.6%, after 24 h of the process.	(9)
Azo dye: RB 19	Biosorption of dyes by white-rot fungus (*Panus tigrinus*). Conditions of the process: initial dye concentration (50–150 mg/L), contact time (30–90 min), and pH (2–6), 15 g/L biosorbent, mixing at 200 rpm.	Concentration of the dye solution measuring by UV-Vis spectrophotometry at 596 nm.	The maximum decolorization of 83.18% at pH 2, a contact time of 90 min, and an initial concentration of 50 mg/L. The minimum decolorization at pH 6, contact time of 30 min, and an initial concentration of 50 mg/L (13.18%).	(43)
Malachite Green and CV	Simultaneous biosorption on fungus biosorbent *Yarrowia lipolytica* ISF7 isolated from wastewater. Conditions of the process: mixing 0.04 g of biomass with solution containing 5–25 mg/L of dyes. Shaking rate of 160 rpm, temperature (15–35°C) and contact times (0–24 h).	Centrifugation at 3000 rpm for 10 min, and analysis of the supernatant by UV/visible spectrophotometer (CV—616 nm, Malachite Green—580 nm).	The maximum biosorption efficiency (>99% for both dyes) at pH 7.0, T = 28°C, 24 h mixing and initial dyes concentrations—20 mg/L.	(17)

Table 2. (*continued*)

Target compound	Experiment setup	Quantification protocols	Complementary data	Ref.
CV and BG[h]	Simultaneous biosorption on live yeast *Yarrowia lipolytica* 70562. Mixing in incubator shakers at 25°C. The best operational conditions: initial CV and BG concentration 8.0 and 10 mg/L, respectively, pH 7.0, and contact time 16 h.	Centrifugation at 4000 rpm for 15 min. Analysis of dye concentration using UV-Vis spectrophotometer. (624 nm for CV and 582 nm for BG).	Maximum biosorption: 98.8% for CV and 99.9% for BG dyes. Maximum biosorption capacity: 65.36 mg/g for BG and 56.5 mg/g for CV.	(10)
Wastewater from a dyeing factory (azo dyes)	Aerobic granules formed from conventional activated sludge with microstructural characteristics potentially suitable for simultaneous anaerobic dye reduction and aerobic mineralization. Procedure: acclimatization with synthetic wastewater (20 days), formation of aerobic granule in the SBR[i] and adaptation to real dyeing wastewater.	Centrifugation at 4200 rpm for 20 min for COD[j] and color measurements. Absorbance of supernatant through visible range (400–700 nm).	73% color removal and 68% COD removal with a cycle time of 24 h and ratio of anaerobic to aerobic period of 3 with adapted granules. Time period of specific aerobic granules obtaining—94 days.	(14)
Basic Red 46—azo colorant	Biosorption of phyco-composite biomaterial composed of *Spirogyra* sp. and *Rhizoclonium* sp. filamentous green algal biomasses. The mix biomass preparation from a freshwater pool. Colorant solution: from 10 to 50 mg/L, weight of biosorbent: 10 mg/100 mL of dye solution, samples periodically shaken at a constant speed at an ambient temperature.	Centrifugation and measurement final concentration of colorant using UV-visible spectrophotometer at the wavelength of 530 nm.	The maximum biosorption capacity of composite biosorbent 56 mg/g. The biosorption capacity of biosorbent decreased as its dosage increased. The biosorption rapidly increases during the first 5 min. Optimum pH for biosorption—9.	(44)
Reactive Orange 16 and Reactive Black 5—azo dyes	Removal by using bacteria *Lactobacillus delbrueckii.* The optimal conditions for dye removal: dye concentration—10 ppm, pH = 6, temperature 37°C, agitation in a rotating orbital shaker at 150 rpm for 48 h.	Measurement of dye concentrations with a spectrophotometer UV-Vis after centrifugation (10 000 rpm, 4°C for 20 min).	Color removal under optimum conditions: 46–60% for Reactive Orange 16 and 49–55% for Reactive Black 5.	(7)
Textile dye industry effluent	MASBR[k]. The ASBR[l] modified by the addition of ground nut shell powder and plastic media as sorbent. The operating procedure of MASBR: Fill—1 h, React—32 h, Settle—2 h, Withdraw—1 h. Time of acclimatization of microorganisms—80 days.	Measurement of dye concentrations using Bio-spectrophotometer (395 nm).	A maximum decolorization of 94.8% and COD reduction of 97.1% for sorbent dosage 10.2 g/L and biomass support 20.2%. The optimal HRT[m] for COD removal efficiency: 6 days. Addition of sorbent and plastic media making decolorization and COD reduction by both processes: biodegradation and adsorption.	(15)

[a] UTCC = Microorganism strain label.

[b] UTEX = Microorganism strain label.

[c] PCC = Microorganism strain label.

[d] AA = Microorganism strain label.

[e] BG-11 = Microorganism strain label.

[f] MN = Microorganism strain label.

[g] CKS6 = Microorganism strain label.

[h] BG = Brilliant Green.

[i] SBR = Sequential batch reactor.

[j] COD = Chemical oxygen demand.

[k] MASBR = Modified anaerobic sequential batch reactor.

[l] ASBR = Anaerobic sequential batch reactor.

[m] HRT = Hydraulic retention time.

ST and CV degradation products can be less toxic to plants compared with parental chemicals (9).

A different group of microorganisms that are important in terms of dye biosorption are fungi. Fungi-driven processes may involve living or dead fungal biomass. The efficiency of this process strongly depends on the properties of the dyes, especially molecular structure and attached ligands. This may finally determine the degree of dye removal from complex wastewater organic matrices (11).

Fungi may produce lignin-degrading enzymes, allowing decomposition and transformation of various chemically resistant polymeric substances (9). Therefore, fungi, compared

with bacteria organisms, can solubilize a number of target substrates that are insoluble in water under typical wastewater processing conditions. This phenomenon has been reported to be important for key wastewater treatment processes including biosorption, bioaccumulation, and biodegradation (43).

It has been found that a large diversity of fungi, especially white-rot fungi, are able to remove a wide range of colorants from wastewaters. Mustafa and coauthors (43) have investigated alternative methods for dye biodegradation using fungal strains. White-rot fungus (*Panus tigrinus*) was used as a biosorbent for the effective decolorization of Reactive Blue 19 (RB 19). The kinetic study revealed that biosorption of the selected dye may occur under the pseudo-second-order kinetic model conditions. Hence, the chemisorption process could be the rate-limiting step of biosorption. They documented that maximum dye removal may be obtained at pH = 2 (reported removal degree equals 83%, approximately). Minimum removal of RB 19 was observed at pH = 4 (removal degree equals 23%, approximately). High removal level of dye at pH = 2 was an effect of electrostatic attraction-driven forces between negatively charged dye anions and the positively charged surface of the fungal biomass. At higher pH, the electrostatic repulsion between biosorbent and dye molecules caused a decrease of the colorant's removal (43).

In recent years, complex biomasses including various green algal organisms have been adapted as biosorptive materials for colorant removal. For example, algal cell walls may consist of a number of functional groups such as hydroxyl, carboxylate, amino, and phosphate. They allow for the removal of dye contaminations from the water phase and enable efficient wastewater decolorization. Moreover, some research indicates that wastewater-generated algae biomass can be the source of a natural and green chemistry biofuel substrate. Generally, the growing interest in algae biosorbents results from their unique biochemical activity and ubiquity in the environment, which is important from an economical point of view (low cost compared with other sorbents and high biosorption of target compounds; 44, 46–48).

Deniz and Ersanli presented experimental data concerning the biosorption properties of a phyco-composite (44). This material was composed of *Spirogyra* sp. and *Rhizoclonium* sp., filamentous green algal biomasses, and applied for removal of Basic Red 46. They investigated the biosorption capacity of algal-derived hybrid composite, which depends on key technological parameters including solution pH, biosorbent mass, dye concentration, and contact time. They have found that the best performance of the hybrid biosorbent studied may be obtained at pH = 9, with the maximum biosorption capacity of 56 mg/g. Interestingly, biosorption of biomass measured using single green algae species was significantly lower in comparison with the hybrid material (44).

Coagulation, Membrane Separation, and Oxidation Processes

Effective wastewater purification from dyes and related pollutants can be performed through processes other than sorption or biodegradation. Particularly, coagulation, membrane separation, and oxidation approaches for wastewater decolorization were successfully investigated and reported. The latest examples of such applications are summarized in Table 3.

Common inorganic coagulants, such as aluminum sulfate, lime, ferric or ferrous sulfate, and polyaluminum chloride (PAC), have been found to be effective reagents for wastewater decolorization. However, the main disadvantage of the application of these coagulants during wastewater treatment is the relatively high cost of chemicals and sludge disposal (49). Therefore, as an alternative to inorganic coagulants, organic polyelectrolytes such as, e.g., polydiallyldimethylammonium chloride and polyamine were proposed. Technological processes involving these chemicals are characterized by low or even no additional sludge production. Moreover, it has been documented that the total amount of such reagents can be much lower in comparison with inorganic coagulants, which may significantly decrease the overall cost of the decolorization processes. Polyelectrolytes have shown negligible sensitivity to pH (ranging from 3 to 10) for almost all types of dye pollutants. Coagulation performed using inorganic coagulants requires stable and narrow pH conditions (e.g., for PAC, pH = 5) to obtain a stable removal rate (47). Another way to reduce the process costs is application of ionic flocculation with low-cost carboxylate surfactants. They are easy to obtain by saponification reaction of vegetable oils and/or animal fats with sodium hydroxide (12).

Important technologies that do not require the use of chemical reagents are based on membrane processes including reverse osmosis, microfiltration, and nanofiltration (NF). They are considered to be cost-effective and time-saving methods (8, 53). Current research has revealed that NF membranes treatment can provide total decolorization of dye-polluted wastewater and may reduce the total salt concentration above 72% (8). The best results of colorant removal were obtained for dyes characterized with a molecule size ranging from 600 to 1000 Da (51).

Membranes can be easily modified with various natural or waste sorptive materials including activated carbons, zeolites, natural polymeric materials, agricultural waste, silicate, clay, and alginates. The resulting hybrid composites are very effective for contaminants separation including dye-related micropollutants. For example, removal of Methylene Blue on the porous calcium alginate membrane under filtration and adsorption modes was investigated by Li and coauthors (13). The alginates extracted from brown algal species have been found to be biocompatible, nontoxic, and nonexpensive. The data presented revealed that filtration properties using the alginate membrane depend on the freeze-drying protocol of membrane preparation and may decrease with an increasing concentration of calcium chloride. Another parameter that was indicated as important is weight ratio of sodium alginate to deionized water. Moreover, the adsorption properties of the porous calcium alginate membrane for target dye were studied, and a number of key experimental parameters were investigated, including pH, contact time, temperature, and adsorbent dosage values. The authors concluded that adsorption of the studied dye was an exothermal process and occurred on the surface of the alginate membrane involving monolayer adsorption. It has been found that optimal filtration properties of the membrane were obtained if the weight ratio of sodium alginate to deionized water was around 1%. For such conditions, more than 90% dye removal was observed (13).

Carbon-based nanomaterials are currently being extensively investigated for various applications, including dye-removal systems. Particularly, graphene and its derivatives are being

Table 3. Removal of dyes from water solutions/wastewater through coagulation, filtration, membrane separation, and other processes

Target compound	Experiment setup	Quantification protocols	Complementary data	Ref.
Direct Yellow 27	Ionic flocculation process by using a mixture of surfactants, produced from animal/vegetable fats. The surfactant was obtained from a mixture of coconut oil and beef tallow. A separating agent (insoluble flocs of calcium surfactant), was obtained by adding a calcium chloride solution to the surfactant solution. Conditions of the process: initial dye concentration—100 ppm, surfactant concentration—from 290 to 650 ppm, calcium/surfactant concentration ratio 1:2, stirring 100 rpm. Sequence: dissolving the surfactant, adding calcium chloride and dye after floc formation.	Dye concentrations before and after experiments were measured by UV–Vis spectrometry.	Dye removal efficiency increased with contact time, achieving up to 90% dye removal after 3 h of contact time. A higher temperature (30–40°C) enhanced the interaction of Direct Yellow 27 with the active sites available onto the calcium surfactant flocs surface.	(12)
Reactive Blue	Coagulation with organic coagulants like poly-DADMAC[a], polyamine with inorganic coagulants such as ferrous sulfate, alum and PAC. Initial concentration of synthetic reactive dye wastes 0.2 g/L of water.	Determining degree of color removal on colorimeter and on a UV-Vis spectrophotometer.	Organic coagulants are more effective in treating reactive dye wastewaters (nearly 100% color removal above 80 ppm dosage). For inorganic coagulants, the color removal efficiency was strongly dependent on pH—(optimum at pH of 5) and for polyamine and poly-DADMAC, pH has no effect on it.	(49)
RB[b]	Fenton and double-cavitating-jets impingement. Conditions of the process: concentrations of RB 33.5 mg/L, 10 mg/L H_2O_2 and 3.33 mg/L $FeSO_4$, temperature 26°C, inlet pressure 10 MPa, pH 3.	UV-spectrophotometric analysis of the dye absorption (554 nm).	85% RB removal by using Fenton and two-cavitating-jets impingement and 34% reduction by only Fenton method (t = 2 h).	(50)
MB[c]	Filtration and the adsorption on the porous calcium alginate membrane. Membrane prepared by a freeze-drying method. MB concentration: 300 mg/L. Optimum conditions of the process: time 4 h, pH 6-10, adsorbent dosages 0.5 g/L.Shaking at a room temperature.	The concentration of the dye detected by a UV-Vis spectrophotometer.	The maximum adsorption capacity of the porous membrane: 3506.4 mg/g. Removal of MB adsorbed by membrane: 96%. Decreasing removal of dye with increasing temperature (15–35°C). Effectivity of the MB removal decreases with decreasing of the pH under 6.1.	(13)
Acid Red Reactive Black Reactive Blue	Reverse osmosis and nanofiltration (NF) membrane. Materials of membranes—composite polyamide, module—spiral wound, active area—7.9 m^2. Operating conditions: dye concentration = 65 mg/L, feed temperature 39°C, and pressure 8 bar.	Dye concentration determination spectrophotometrically (wavelength: Acid Red 500 nm, Reactive Black 600 nm, Reactive Blue 570 nm).	Dye removal with reverse osmosis membrane: 97.2%—Acid Red, 99.58%—Reactive Black, and 99.9%—Reactive Blue. Efficiency of NF membrane: 93.77%—Acid Red, 95.67%—Reactive Black, and 97%—Reactive Blue removal. Effect order of the operating variables on dye removal of membranes: concentration > pH > pressure > TDS[d].	(8)
Acid dye Reactive dye	PES[e] ultrafiltration membrane coated with PVA[f] to give thin-film nanofiltration membranes by dip-coating method. Crosslinking PVA on the surface by using Malic acid. PVA concentration at 1%. A dyes concentration of 100 mg/L, pressure between 5 atm and 15 atm, pH of 3, 7, and 11. Membrane filtration in cross-flow membrane setup.	Measurement of dye concentration by UV-Vis spectrophotometer. The wavelength for the maximum absorbance was found for each dye.	Maximum rejection for disperse dye 97.78% at 15 atm. Maximum rejection values for acid dye 95.7% and reactive dye 93.5%. More rejection of acid dye on basic condition. Positive effect of feed concentration on rejection for reactive dyes. With increasing pH values (from 3 to 11), the acid dye rejection increased from 78 to 95.7%.	(51)

Table 3. (*continued*)

Target compound	Experiment setup	Quantification protocols	Complementary data	Ref.
Reactive Red 141	Modified PVDF[g]/Brij-58 blend nanofiltration membranes. Brij-58 surfactant used as a hydrophilic additive to improve water permeation and fouling resistance of membranes. Operating conditions: room temperature (25°C), trans-membrane pressure of 6 bar, dye concentration of 15 ppm.	Determining the dye concentration in feed and permeate solutions by a UV-Vis spectrophotometer at a wavelength of 545 nm.	Addition of Brij-58 to increase porosity and fouling resistance as well as higher water permeation flux but worse dye rejection values during filtration. The rejection of dye decreased negligibly after addition of Brij-58 from 94% for the pristine membrane to 90% for the membrane containing 4 wt.% Brij-58.	(52)
Indigo	OMWCNTs[h]-PAN[i]/PP[j] composite membranes. The hierarchical composite membrane comprising OMWCNTs functional layer built via electrospraying, ultrathin electrospun PAN midlayer, and microfibrous PP nonwoven support. Conditions of the process: concentrations of dye 20 mg/L, a crossflow filtration system with a pressure of 0.1 MPa.	Treating of suspensions by centrifugation and the measuring of dye concentration by UV-Spectrophotometer.	Dye rejection ratio 98.73% and water flux 3891.85 L/m^2 h. The dye rejection ratios of composite membranes increased gradually when the additive amount of OMWCNTs increased. Process principle of the high rejection ratios: multilevel blocking, sieving, and adsorptive action.	(53)
Congo Red, RB, Methyl Orange, and MB	Graphene oxide framework-based membranes separation with high-flux (GO-IPDI membranes). The effective area of a cross-linked GO-IPDI membrane sample—12.56 cm^2, dyes concentration 10 mg/L, dyes feed solution 10 mL, pressure 1 bar, and pH 7.	The dye concentration in the permeate solution measured by UV-Vis spectrophotometer (wavelength range of 200–700 nm).	The rejection rate of GO-IPDI membranes: MB—97.6, RB—96.2, Methyl Orange—96.9, and Congo Red—98.2%. The rejection rate of GO-IPDI membranes for organic dye molecules is not depended on pH. The flux membrane of 80–100 $L/m^2 \cdot h \cdot bar$ under an extremely low external pressure (1.0 bar). The zeta potential of GO-IPDI membrane:–15.79 mV at 25°C, pH 7).	(54)
Reactive Red 195 (azo anionic dye)	Photo-Fenton-like process. Catalyst: BFD[k] containing hematite, magnetite, and maghemite as iron sources. Source of light: 80 W Hg lamp emitting at 240 nm. Oxidation conditions: dye solution 100 mg/L, BFD 1 g/L, pH 3.0 ± 0.2; temperature 25°C; H_2O_2 was added after 24 h of storage of the sample in the dark.	The concentration of dye was measured spectrophotometrically at 517 nm, while concentration of iron was measured by AAS[l] and by spectrophotometric 1,10-phenanthroline method.	Low cost of catalyst (waste), its high density and magnetic properties, which allow easy solid–liquid separation as well as high catalytic activity, make BFD a versatile material for environmental applications.	(55)
Congo Red, Methylene Blue, and Methyl Orange	Reduction process. Catalyst: graphene oxide covered by platinum nanoparticles. Reduction conditions: 5 g catalyst, 25 mL dye solution (10 ppm), 25 mL $NaBH_4$ (5.3 mM), stirring at room temperature.	Separation of catalyst by centrifugation and spectrophotometric analysis of Congo Red, Methyl Orange, and Methylene Blue at 493, 465, and 663 nm, respectively.	Short time of reduction. After washing with ethanol, catalyst can be reused without significant decrease in catalytic activity.	(56)
Orange G (azo dye)	Degradation in the integrated system: microbial reverse-electrolysis conjugated with electro-Fenton process Oxidation conditions: concentration of dye 400 mg/L, pH 2, aeration of catholyte 8 mL/min, temperature 22 ± 2°C.	The concentration of dye was determined by a UV-Vis spectrophotometry at 478 nm, while its mineralization rate was determined on the base of TOC[m] analysis.	This novel technology is an efficient and cost-effective method for the degradation of nonbiodegradable pollutants. Almost whole mineralization of dye was achieved after 10 h with very low energy consumption—25.93 kWh/ (kg TOC).	(57)
MB	Adsorption combined with photocatalysis process. Solution of MB was irradiated with UV in the presence of trititanate nanotubes with different sodium contents. Oxidation conditions: 0.02 g catalyst, 150 mL dye solution (20 ppm), irradiation with Hg lamp (λ = 254 nm, Io = 4400 $\mu W/cm^2$), temperature 20°C.	The solution of dye was filtered (0.22 μm) and analyzed in a UV-Vis spectrophotometer at 664 nm. Degree of dye mineralization was determined by decrease of TOC.	The mechanism of dye removal strongly depends on sodium content in the nanotubes—a high content of Na dominates the adsorption process (mainly by cation exchange mechanism), but in the case of hydrogen nanotubes, dye oxidation by OH· radical is preferred.	(58)

Table 3. (*continued*)

Target compound	Experiment setup	Quantification protocols	Complementary data	Ref.
Rhodamine B	Removal of dye (from aqueous solution of dye in the presence of sodium sulfate) through membrane separation on coal-based membranes with pore size of 0.382 μm, coupled with electrochemical degradation.	The concentration of Rhodamine B was analyzed spectrophotometrically at 554 nm, while N-di-ethylated intermediates of oxidation were detected by HPLC/MS.	The presence of an electric field enhanced the permeability and efficiency of oxidation, especially under acidic conditions.	(59)
Reactive Red 195 (azo dye)	Adsorption on polyacrylonitrile nanofibrous membrane, modified with hydrazine hydrate and hydroxylamine, coordinated with Fe^{3+} ions. Simultaneously, the adsorbent was a heterogeneous catalyst of Fenton process. Oxidation conditions: 0.10 g catalyst, 50 mL dye solution (0.10 mmol/L), pH 6.0; after 10 h of dark adsorption, H_2O_2 was added to the mixture (6 mmol/L), irradiation with Hg lamp (λ > 420 nm, Io = 8.42 mW/cm^2), temperature 25°C.	The concentration of dye was analyzed by a UV-Vis spectrophotometry at 522 nm.	The fabricated nanofibrous materials were chemically stable, so they could be reused. The synergistic adsorption-photocatalysis processes increased removal of dye.	(60)

[a] DADMAC = Diallyldimethylammonium chloride.

[b] RB = Rhodamine B.

[c] MB = Methylene Blue.

[d] TDS = Total dissolved solids.

[e] PES = Polyethersulfone.

[f] PVA = Poly(vinyl alcohol).

[g] PVDF = Polyvinylidene fluoride.

[h] OMWCNTs = Oxidized multi-wall carbon nanotubes.

[i] PAN = Polyacrylonitrile.

[j] PP = Polypropylene.

[k] BFD = Blast furnace dust.

[l] AAS = Atomic absorption spectrometry.

[m] TOC = Total organic carbon.

tested as highly selective adsorption materials and permeable filtration membrane components. Figure 4 presents the significant increase in the number of publications concerning graphene application to dye wastewater treatment in the last 5 years. These materials are characterized by high mechanical strength and chemical resistance (54). Interaction mechanisms of graphene-based nanomaterials with low-molecular-mass compounds are studied under various experimental conditions, also involving living organisms or isolated cells and tissues (61–66). Particularly, high retention of organic dyes and moderate retention of ion salts on ultrathin (22–53 nm thick) graphene nanofiltration membranes can be observed. Graphene oxide (GO) membranes have revealed an ability for specific removal of water and wastewater pollutants. These systems can be prepared by using various procedures that alter their permeability and may finally reduce the rejection rate. Simple and effective methods for graphene oxide framework membrane modifications by cross-linking with isophorone diisocyanate (IPDI) have been developed by Zhang and coauthors (54). They reported that a purification process involving a cross-linked GO-IPDI membrane successfully eliminated more

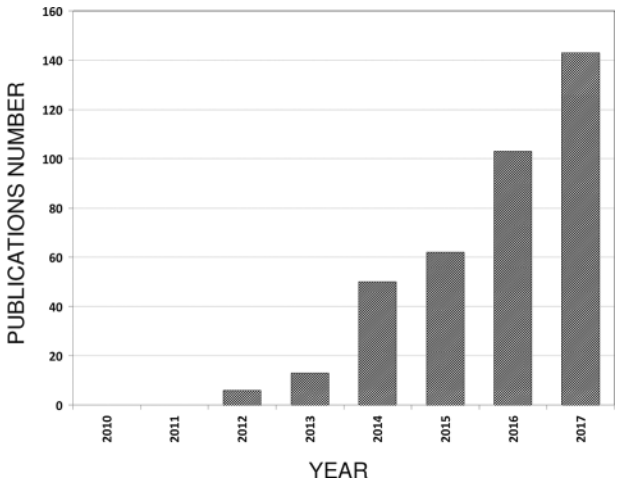

Figure 4. Comparison of the number of manuscripts available through the Web of Science database by year, related to topic key words search: "dye" and "wastewater" and "graphene."

than 96% of tested dyes (Methylene Blue, Methylene Orange, Rhodamine-B, and Congo Red). The rejection rate was stable under various pH conditions and flux values ranging from 80 to 100 L m^{-2} h^{-1} bar^{-1} measured under low external pressure (1.0 bar; 53).

In the case of the above-described coagulation, filtration, sorption, or membrane separation-driven purification processes, given pollutants are transferred to another phase. Therefore, new waste products may be generated, and, consequently, additional waste-treatment processes must be involved. As alternative methods, causing partial or total mineralization of target pollutants, the advanced oxidation processes (AOPs), including Fenton and Fenton-like processes (61, 67, 68) as well as photocatalysis with nanostructured catalysts (64), were proposed. Under such conditions, degradation of dyes through intermediates to mineralization products, such as carbon dioxide and water, can be expected.

Liu and coworkers (68) synthesized a new nanocomposite involving α-Fe_2O_3 particles and graphene oxide molecules to degrade various cationic and anionic dyes (Methylene Blue, Rhodamine B, Orange II, Orange G) and selected neutral compounds including endocrine disrupter (phenol, 2-nitrophenol, 17β-estradiol) via heterogeneous photo-Fenton process. This approach is very promising because of its high efficiency, wide range of pH solution applied, and overall catalyst durability. In this particular case, incorporation of graphene oxide to the catalyst body had a significant impact on active site location (surface of α-Fe_2O_3 particles) and increase of electron conductivity as well as electrostatic attraction between negatively charged catalyst surface and cationic Methylene Blue. The authors reported that high efficient degradation (around 96–100%) was obtained for both cationic and anionic dyes.

Conclusions

The efficient removal of dye micropollutants from industry-originated wastewaters is still considered to be a difficult task. This is because of the potential hazard of target components to the environment and the high cost of elimination processes. A number of dye-removal technologies based on (*1*) physicochemical (adsorption, ion exchange, filtration, and coagulation), (*2*) chemical (AOPs, photocatalytic reactions, ozonization), and (*3*) biological processes (aerobic and anaerobic degradation, biosorption) are still commonly applied and developed. They are characterized by several advantages and disadvantages, which are summarized in Table 4.

Adsorption is used as the main process for dye removal from industrial sewage, especially using popular adsorbents such as activated carbon. However, this material has been gradually replaced by other sorbents, based on agricultural and industrial waste characterized by dyes' high affinity (e.g., compounds extracted from orange bagasse, fungus biosorbent, or green algal biomasses). Chemical and biological methods are efficient but have several limitations as they often must involve high investment and operational costs. Ultra- and nanofiltration methods are becoming increasingly important as alternative treatment methods for colored wastewater. Membrane methods have higher removal potential with lower effective cost in comparison with, e.g., biological treatment systems.

New decolorization materials are extensively invented, particularly those based on carbon nanomaterials (carbon nanotubes or graphene oxide working as adsorbent, catalyst, or membrane component). These materials, which are frequently combined with magnetic particles, allow efficient mechanical separation of adsorbed pollutants after dye-removal treatment. It should be noted that the problem of handling and disposing

Table 4. Summary of advantages and disadvantages of various methods used for dye wastewater treatment

Technology	Advantages	Disadvantages
Physicochemical methods		
Adsorption on commercial activated carbon	High removal efficiency.	High cost of sorbent and its regeneration; the loss of AC[a] during regeneration.
Adsorption on waste-based sorbents	Low cost and availability of adsorbent.	Lower sorption capacity compared with activated carbon. Requires modification.
Coagulation/flocculation	Simple and low-cost methodology. High removal efficiency.	Handling and disposal problems due to high sludge production. High cost of chemical reagent.
Membrane separation	High removal efficiency, regardless of the type of dye.	Expensive, requires high pressure. Used mainly in small installation. Production of concentrated sludge.
Chemical methods		
Fenton-like process	High removal efficiency, regardless of the type of dye.	High operational and investment costs. Generation of byproduct.
Ozonation	Rapid and efficient process. Ozone as a gas does not increase a treated volume.	Low stability of oxidant. Hazardous byproducts are formed. Ozone destructive unit is required.
Biological methods		
Biodegradation	Economically attractive. Technology considered a green and pro-ecological treatment.	Effectiveness of process strongly depends on kind of dyes. Slow process, requires maintaining optimal process conditions and nutrients addition.

[a] AC = Activated carbon.

of the sludge mass, which is vastly produced, especially during treatment methods based on coagulation and flocculation processes, is still unsolved.

References

(1) Kant, R. (2012) *Natural Sci*. **4**, 22–26. doi:10.4236/ns.2012.41004
(2) Kuppusamy, S., Sethurajan, M., Kadarkarai, M., & Aruliah, R. (2017) *J. Environ. Chem. Eng.* **5**, 716–724
(3) Hamdaoui, O., Saoudi, F., Chiha, M., & Naffrechoux, E. (2008) *Chem. Eng. J.* **143**, 73–84
(4) Barka, N., Abdennouri, M., & Makhfouk, M.E. (2011) *J. Taiwan Inst. Chem. Eng.* **42**, 320–326
(5) 2016 World's Worst Pollution Problems, Published by Green Cross Switzerland and Pure Earth Report, http://www.worstpolluted.org
(6) Croce, R., Cinà, F., Lombardo, A., Crispeyn, G., Cappelli, C.I., Vian, M., Maiorana, S., Benfenati, E., & Baderna, D. (2017) *Ecotoxicol. Environ. Saf.* **144**, 79–87. doi:10.1016/j.ecoenv.2017.05.046
(7) Siti Zuraida, M., Nurhaslina, C.R., & Ku Halim, K.H. (2013) *IRJES* **2**, 1–7
(8) Abid, M.F., Zablouk, M.A., & Abid-Alameer, A.M. (2012) *J. Environ. Health Sci. Eng.* **9**, 1–9. doi:10.1186/1735-2746-9-17
(9) Buntić, A.V., Pavlović, M.D., Antonović, D.G., Šiler-Marinković, S.S., & Dimitrijević-Branković, S.I. (2017) *J. Clean. Prod.* **148**, 347–354
(10) Dil, E.A., Ghaedi, M., Reza, G., & Asfaram, A. (2017) *Ecotoxicol. Environ. Saf.* **139**, 158–164
(11) Rybczyńska-Tkaczyk, K., & Korniłłowicz-Kowalska, T. (2016) *Int. J. Environ. Sci. Technol.* **13**, 2837–2846. https://doi.org/10.1007/s13762-016-1111-3
(12) Melo, R.P.F., Barros Neto, E.L., Moura, M.C.P.A., Castro Dantas, T.N., Dantas Neto, A.A., & Nunes, S.K.S. (2017) *J. Surfact. Deterg.* **20**, 459–465
(13) Li, Q., Li, Y., Ma, X., Du, Q., Sui, K., Wang, D., Wang, C., Li, H., & Xia, Y. (2017) *Chem. Eng. J.* **316**, 623–630
(14) Manavi, N., Kazemi, A.S., & Bonakdarpour, B. (2017) *Chem. Eng. J.* **312**, 375–384
(15) Rajasimman, M., Venkatesh Babu, S., & Rajamohan, N. (2017) *J. Taiwan Inst. Chem. Eng*. **72**, 171–181. https://doi.org/10.1016/j.jtice.2017.01.027
(16) Janović, B.S., Collins, A.R., Vujčić, Z.M., & Vujčić, M.T. (2017) *J. Hazard. Mater.* **321**, 576–585. doi:10.1016/j.jhazmat.2016.09.037
(17) Asfaram, A., Ghaedi, M., Ghezelbash, G.R., & Pepe, F. (2017) *Ecotoxicol. Environ. Saf.* **139**, 219–227
(18) Zhao, X., Kai Ma, K., Jiao, T., Xing, R., Ma, X., Hu, J., Huang, H., Zhang, L., & Yan, X. (2017) *Sci. Rep.* **7**, 1–13. doi:10.1038/srep44076
(19) Zhang, Y., Huang, G., An, C., Xin, X., Liu, X., Raman, M., Yao, Y., Wang, W., & Doble, M. (2017) *Sci. Total Environ.* **595**, 723–732
(20) Tang, J., Mu, B., Zong, L., Zheng, M., & Wang, A. (2017) *Chem. Eng. J*. **322**, 102–114. https://doi.org/10.1016/j.cej.2017.03.116
(21) Moawed, E.A., El-Hagrasy, M.A., & Farhat, A.A.M. (2017) *J. Clean Prod.* **157**, 232–242
(22) Ansari, M.O., Kumar, R., Ansari, S.A., Ansari, S.P., Barakat, M.A., Alshahrie, A., & Cho, M.H. (2017) *J. Colloid Interface Sci.* **496**, 407–415. doi:10.1016/j.jcis.2017.02.034
(23) Wang, W., Liu, L., Jiang, X., Yu, J., & Chen, X. (2015) *Colloid Surf. A* **466**, 166–173
(24) Li, N., & Lei, X.L. (2012) *J. Incl. Phenom. Macrocycl. Chem.* **74**, 167–176. doi:10.1007/s10847-011-0096-2
(25) Nesic, A.R., Kokunesoski, M.J., Volkov-Husovic, T.D., & Velickovic, S.J. (2016) *Environ. Monit. Assess*. **188**, 160. doi:10.1007/s10661-016-5155-0
(26) Khosravi, M., & Azizian, S. (2014) *J. Ind. Eng. Chem.* **20**, 2561–2567. https://doi.org/10.1016/j.jiec.2013.10.040
(27) Bensalah, H., Bekheet, M.F., Younssi, S.A., Ouammou, M., & Gurlo, A. (2017) *J. Environ. Chem. Eng.* **5**, 2189–2199
(28) Lessa, E.F., Gularte, M.S., Garcia, E.S., & Fajardo, A.R. (2017) *Carbohydr. Polym.* **157**, 660–668. doi:10.1061/j.carbpol.2016.10.019
(29) Issa, A.A., Abdel-Halim, H.M., Al-Degs, Y.S., & Al-Masri, H.A. (2017) *Res. Chem. Intermed.* **43**, 523–544
(30) Namvari, M., & Namazi, H. (2016) *Int. J. Environ. Sci. Technol.* **13**, 599–606
(31) Zarzycki, P.K., Fenert, B., & Głód, B.K. (2016) in *Encapsulations, Nanotechnology in the Agri-Food Industry*, Vol. 2, Elsevier, London, United Kingdom, Ch. 17, pp 717–767
(32) Crini, G. (2005) *Prog. Polym. Sci*. **30**, 38–70. https://doi.org/10.1016/j.progpolymsci.2004.11.002
(33) Adams, F.V., Nxumalo, E.N., Krause, R.W.M., Hoek, E.M.V., & Mamba, B.B. (2014) *Phys. Chem. Earth* **67–69**, 71–78. https://doi.org/10.1016/j.pce.2013.11.001
(34) Sanchez-Trujillo, M., Lacorte, S., Villaverde, J., Barata, C., & Morillo, E. (2014) *Environ. Sci. Pollut. Res. Int.* **21**, 507–517. doi:10.1007/s11356-013-1930-4
(35) Han, J., Xie, K., Du, Z., Zou, W., & Zhang, C. (2015) *Carbohydr. Polym.* **120**, 85–91. doi:10.1016/j.carbpol.2014.12.011
(36) Khaoulani, S., Chaker, H., Cadet, C., Bychkov, E., Cherif, L., Bengueddach, A., & Fourmentin, S. (2015) *C. R. Chim.* **18**, 23–31
(37) Pérez-Álvarez, L., Matas, J., Gómez-Galván, F., Ruiz-Rubio, L., León, L.M., & Vilas-Vilela, J.L. (2017) *Carbohydr. Polym.* **156**, 143–151. doi:10.1016/j.carbpol.2016.09.020
(38) Varaprasad, K., Jayaramudu, T., & Sadiku, E.R. (2017) *Carbohydr. Polym.* **164**, 186–194. doi:10.1016/j.carbpol.2017.01.094
(39) Ge, M., Du, M., Zheng, L., Wang, B., Zhou, X., Jia, Z., Hu, G., & Alam, S.M.J. (2017) *Mater. Chem. Phys.* **192**, 147–155
(40) Peláez-Cid, A.A., Herrera-González, A.M., Salazar-Villanueva, M., & Bautista-Hernández, A. (2016) *J. Environ. Manage.* **181**, 269–278. doi:10.1016/j.jenvman.2016.06.026
(41) Marrakchi, F., Ahmed, M.J., Khanday, W.A., Asif, M., & Hameed, B.H. (2017) *J. Taiwan Inst. Chem. E* **71**, 47–54
(42) Dellamatrice, P.M., Silva-Stenico, M.E., Beraldo de Moraes, L.A., Fiore, M.F., & Rosim Monteiro, R.T. (2017) *Braz. J. Microbiol.* **48**, 25–31
(43) Mustafa, M.M., Jamal, P., Alkhatib, M.F., Mahmod, S.S., Jimat, D.N., & Ilyas, N.N. (2017) *Electron. J. Biotechnol.* **26**, 7–11
(44) Deniz, F., & Ersanli, E.T. (2016) *J. Mol. Liq*. **220**, 120–128. https://doi.org/10.1016/j.molliq.2016.04.081
(45) Chen, K.C., Wu, J.Y., Liou, D.J., & Hwang, S.C. (2003) *J. Biotechnol.*, **101**, 57–68
(46) Piaskowski, K., Świderska-Dabrowska, R., Kaleniecka, A., & Zarzycki, P.K. (2017) *J. AOAC Int.* **100**, 962–970. doi:10.5740/jaoacint.17-0170
(47) Zarzycki, P.K., Kaleniecka, A., Fenert, B., & Zarzycka, M.B. (2017) *Stud. Nat. Prod. Chem.* **54**, 87–107. http://dx.doi.org/10.1016/B978-0-444-63929-5.00003-6
(48) Zarzycki, P.K., & Portka, J.K. (2015) *J. Steroid Biochem. Mol. Biol.* **153**, 3–26. doi:10.1016/j.jsbmb.2015.04.017
(49) Ashtekar, V.S., Bhandari, V.M., Shirsath, S.R., Sai Chandra, P.L.V.N., Jolhe, P.D., & Ghodke, S.A. (2014) *Jr. Ind. Poll. Cont.* **30**, 33–42
(50) Tao, Y., Cai, J., Huai, X., & Liu, B. (2017) *J. Hazard. Mater.* **335**, 188–196. doi:10.1016/j.jhazmat.2017.04.046
(51) Babu, J., & Murthy, Z.V.P. (2017) *Sep. Purif. Technol.* **183**, 66–72. doi:10.1016/j.seppur.2017.04.002
(52) Nikooe, N., & Saljoughi, E. (2017) *Appl. Surf. Sci.* **413**, 41–49

(53) Xu, Z., Li, X., Teng, K., Zhou, B., Ma, M., Shan, M., Jiao, K., Qian, X., & Fan, J. (2017) *J. Membr. Sci.* **535**, 94–102
(54) Zhang, P., Gong, J.L., Zeng, G.M., Deng, C.H., Yang, H.C., Liu, H.Y., & Huan, S.Y. (2017) *Chem. Eng. J.* **322**, 657–666
(55) Amorim, C.A., Leao, M.M.D., Moreira, R.F.P.M., Fabris, J.D., & Henriques, A.B. (2013) *Chem. Eng. J.* **224**, 59–66
(56) Omidvar, A., Jaleh, B., & Nasrollahzadeh, M. (2017) *J. Colloid Interface Sci.* **496**, 44–50. doi:10.1016/j.jcis.2017.01.113
(57) Li, X., Jin, X., Zhao, N., Angelidaki, I., & Zhang, Y. (2017) *Bioresour. Technol.* **228**, 322–329. doi:10.1016/j.biortech.2016.12.114
(58) Sandoval, A., Hernández-Ventura, C., & Klimova, T. E. (2017) *Fuel* **198**, 22–30
(59) Tao, P., Xu, Y., Song, C., Yin, Y., Yang, Z., Wena, S., Wanga, S., Liu, H., Li, S., Li, C., Wang, T., & Shao, M. (2017) *Sep. Purif. Technol.* **179**, 175–183
(60) Li, F., Dong, Y., Kang, W., Cheng, B., & Cui, G. (2017) *Appl. Surf. Sci.* **404**, 206–215
(61) Dybowska-Sarapuk, Ł., Kotela, A., Krzemiński, J., Wróblewska, M., Marchel, H., Romaniec, M., Łęgosz, P., & Jakubowska, M. (2017) *J. AOAC Int.* **100**, 900–904. doi:10.5740/jaoacint.17-0164
(62) Niemiec, T., Dudek, M., Dziekan, N., Jaworski, S., Przewozik, A., Soszka, E., Koperkiewicz, A., & Koczoń, P. (2017) *J. AOAC Int.* **100**, 905–915. doi:10.5740/jaoacint.17-0165
(63) Czerniak-Reczulska, M., Niedzielski, P., Balcerzyk, A., Bartosz, G., Karowicz-Bilińska, A., & Mitura, K. (2010) *J. Nanosci. Nanotechnol.* **10**, 1065–1071. doi:10.1166/jnn.2010.1851
(64) Kurantowicz, N., Strojny, B., Sawosz, E., Jaworski, S., Kutwin, M., Grodzik, M., Wierzbicki, M., Lipińska, L., Mitura, K., & Chwalibog, A. (2015) *Nanoscale Res. Lett*. **10**, 398. doi:10.1186/s11671-015-1107-9
(65) Kurantowicz, N., Sawosz, E., Jaworski, S., Kutwin, M., Strojny, B., Wierzbicki, M., Szeliga, J., Hotowy, A., Lipińska, L., Koziński, R., Jagiełło, J., & Chwalobog, A. (2015) *Nanoscale Res. Lett*. **10**, 23. doi:10.1186/s11671-015-0749-y
(66) Mitura, K., Wyrębski, K., & Zarzycki, P.K. (2017) in *Food Packaging, Nanotechnology in the Agri-Food Industry*, Vol. 7, Elsevier, London, United Kingdom, Ch. 9, pp 295–328
(67) Świderska-Dąbrowska, R., & Piaskowski, K., (2009) *Pol. J. Environ. Stud.* **2**, 68–73
(68) Liu, Y., Jin, W., Zhao, Y., Zhang, G., & Zhang, W. (2017) *Appl. Catal. B-Environ.* **206**, 642–652